



# Investigation of $^{209}\text{Bi}(\alpha,2n)^{211}\text{At}$ reaction route for the production of $\alpha$ -emitter $^{211}\text{At}$

Hasan Özdogan<sup>1,a</sup>, Yiğit Ali Üncü<sup>2</sup>, Mert Şekerci<sup>3</sup>, Abdullah Kaplan<sup>3</sup>

<sup>1</sup> Department of Medical Imaging Techniques, Vocational School of Health Services, Antalya Bilim University, 07190 Antalya, Turkey

<sup>2</sup> Department of Biomedical Equipment Technology, Vocational School of Technical Sciences, Akdeniz University, 07070 Antalya, Turkey

<sup>3</sup> Department of Physics, Süleyman Demirel University, 32260 Isparta, Turkey

Received: 21 January 2024 / Accepted: 27 May 2024  
© The Author(s) 2024

**Abstract** In this research, the calculations have been done for  $\alpha$ -emitters of  $^{211}\text{At}$ , which is a promising isotope in cyclotrons for radiotherapy. The scope of the study is to investigate the production parameters of  $^{211}\text{At}$ , which can be produced in the cyclotron by bombarding bismuth with an alpha particle beam for the  $^{209}\text{Bi}(\alpha,2n)^{211}\text{At}$  reaction. The total activity, reaction yield, and production cross-sections of  $^{209}\text{Bi}(\alpha,2n)^{211}\text{At}$  reaction have been calculated by using diverse level density models of the TALYS 1.95 code. Furthermore, recommended data with 95% confidence limits have been obtained. Experimental data available in the literature based on EXFOR compilation are used to compare the findings. Consequently, the required beam energy has been found to be 28 MeV to produce  $^{211}\text{At}$ .

## 1 Introduction

In the field of nuclear medicine, which is supported by the studies of researchers from different disciplines such as biology, biomedical, biophysics, clinicians, medical physicists, pharmacologists, radiochemists, a significant portion is devoted to studies for curative therapy, disease control, or palliation. The number of therapeutic radioisotopes available, including alpha, beta, and Auger electron emission, has increased significantly over the last century as a result of field research to improve applications. The primary goal for these advancements may be demonstrated as maximizing treatment success by matching the particle degradation mechanism, effective range, and relative biological activity to tumor bulk, size, radiosensitivity, and heterogeneity [1].

The particle called alpha is a bare  $^4\text{He}$  nucleus with + 2 charge. The initial kinetic energy of monoenergetic alpha particles is typically between 5 and 9 MeV and, as a result of this amount of kinetic energy, they have a penetrating distance of 50 to 100  $\mu\text{m}$ . Due to their mass, the alpha particles deviate less than the electrons, and their direction of motion is usually almost linear [2]. Alpha particles, which are known to be effective ionizing agents, are also classified as particles that provide high linear energy transfer (LET). Because alpha particles cannot be directly observed *in vivo*, gamma rays, distinct X-rays, or bremsstrahlung radiation produced by radionuclide decay are frequently used to assess target uptake, dosimetry, and therapeutic response [3, 4].

In addition to the availability of radioisotopes, their physical properties such as half-lives may limit their distribution in a wide range of uses. The  $\alpha$ -emitters radionuclides are known for high cell-killing efficiency. Although it is known that there are many types of radionuclides that decay by particle emission, it is possible that only a few of them can be used for medical purposes. The alpha particles have substantially higher LET values than photons and beta particles. Furthermore, their ability to damage the cells by producing double-strand breaks is a significant feature that distinguishes them from other beams in terms of delivering more harm to targeted cancer cells [5]. The alpha particles lose more energy (approximately 100–1000 times) while they pass through DNA than conventional external X-ray radiation or beta particles [6].

Radionuclide treatment frequently employs astatine-211 ( $^{211}\text{At}$ ), an alpha-emitting radionuclide [7]. It is possible to produce  $^{211}\text{At}$  in the cyclotron using the  $^{209}\text{Bi}(\alpha,2n)^{211}\text{At}$  reaction. The  $^{211}\text{At}$  isotope has a half-life of 7.2 h, which presents many opportunities for positive outcomes in the context of targeted alpha particle treatment. The nuclear reaction  $^{209}\text{Bi}(\alpha,2n)^{211}\text{At}$  can produce  $^{211}\text{At}$  from bismuth targets in a yield that is satisfactory by using uncomplicated processes [8].

$^{211}\text{At}$  possesses several features that are suited for targeted alpha particle radiotherapy in addition to its half-life, which makes it an ideal candidate for that application. The emission of an alpha particle is associated with one hundred percent of the decays of  $^{211}\text{At}$ . This can occur either through a direct alpha decay to  $^{207}\text{Bi}$  (42%) followed by an electron capture decay to stable  $^{207}\text{Pb}$  or through a beta decay to  $^{211}\text{Po}$  (58%), followed by alpha emission to stable  $^{207}\text{Pb}$ . The possibility of radioactivity from the  $^{211}\text{At}$  absorption and decay site escaping into the environment is a possible issue that is related to the second decay branch. However,

<sup>a</sup> e-mail: [hasan.ozdogan@antalya.edu.tr](mailto:hasan.ozdogan@antalya.edu.tr) (corresponding author)

the issue is not nearly as serious as the one that is associated with  $^{225}\text{Ac}$ 's radioactive daughters, which emit alpha particle with a much longer half-life. This is due to the fact that the half-life of the  $^{211}\text{Po}$  is on an intermediate level, which is 520 ms, thereby limiting the diffusion distance before the emission of alpha particle. Furthermore, the potentially destabilizing influence of alpha particle recoil nuclei on chemical stability is irrelevant since  $^{211}\text{Po}$  is not a product of alpha decay. The second branch of decay, which involves electron capture, ultimately results in the emission of polonium K X-rays with energies ranging from 77 to 92 keV, which is a substantial benefit for  $^{211}\text{At}$  [9].

$^{211}\text{At}$  decays to stable  $^{207}\text{Pb}$  via a branched pathway with a half-life of 7.2 h. With it decays to  $^{211}\text{Po}$ ,  $^{211}\text{At}$  emits K-shell x-rays, allowing for in vivo sample counting and scintigraphy of  $^{211}\text{At}$  in the thyroid, stomach, and macrophage-bearing organs such as the spleen and lung [10]. The following sections analyze the production routes and parameters of  $^{211}\text{At}$  in three parts; determining beam energy, production cross-section calculations, activation, and yield calculations. The TALYS 1.95 [10] code has been utilized to calculate each of the parameters that are discussed in this paper.

## 2 Material and methods

Calculating the outcome of a nuclear reaction requires the utilization of a significant number of interconnected models, the quality and validity of which are, for the most part, well understood. The optical model and the compound nucleus model are the two models that have been used ever from the very beginning of the study of nuclear processes. Both of these models are still in use today. It is generally agreed that these two models are the earliest ones in the collection. When it relates to the amount of time needed for a nuclear reaction to occur, both models apply to two extreme instances. The interaction between a projectile and a target that takes place in the smallest length of time is represented by the optical model, whereas the compound nucleus model represents the interaction process that occurs over the longest amount of time. This model corresponds to the scenario in which the projectile has been absorbed into the target and has shared its energy with the constituents of the target.

TALYS is comprised of a very wide selection of models. In the computations, some of these will be used automatically. Cross sections, angular distributions, double differential spectra, prompt neutron multiplicities, and other nuclear reaction data can all be calculated using TALYS code. These calculations are necessary for understanding nuclear reactions. The elastic, capture, inelastic, and fission cross sections are the required cross sections that must be considered in order to remain consistent with the aforementioned characteristics.

All of the TALYS computations, including the default and the altered ones, were completed by using TALYS 1.95 code. Modifications were made to the TALYS parameters in order to establish a sufficient agreement between the predicted total and partial cross sections and the results of the experiments. In most of the cases, 10–20 of the TALYS input parameters will need to be adjusted and then recorded in a database for each nuclide target. The most frequently altered parameters include the real volume radius and diffuseness of the optical model, particle-hole state density parameters for the pre-equilibrium process, total level density parameters for the compound and residual nuclides, and knockout and stripping parameters to significantly change the cross-sections. The particle-hole state density parameters for the pre-equilibrium phase, the overall level density parameters of the compound, and residual nuclides are other characteristics that are regularly modified [10].

As level density models, the Constant Temperature Fermi Gas Model (FGM), the Back-Shifted Fermi Gas Model (BSFGM), and the Generalised Superfluid Model (GSM) were chosen to be used in the computations that were included in the scope of the research. During the process of calculating the cross section, the Two Component Exciton Model was used. The nuclear state is represented by the sum of the total energy at any given instant throughout the reaction in the Two Component Exciton Model. Additionally, the nuclear state is characterized by the sum of the particles ( $p$ ) that are above the Fermi surface and the holes ( $h$ ) that are below it. In this model, it is assumed that all of the available pathways have an equal likelihood of sharing excitation energy across various states of particles and holes that have the same number of excitons ( $n = p + h$ ) [11–13].

To validate these models and ensure data consistency, a theoretical approach was employed to analyze experimental data. The assessment method utilized a theoretical approach to analyze experimental data, as referenced in several prior studies [14–16]. This process included two main phases: i) performing nuclear model-based cross section calculations to ensure data consistency, and ii) applying a polynomial function to fit the chosen data. Initially, the experimental cross-section to model-based calculation ratio ( $\sigma_{\text{exp}}/\sigma_{\text{model}}$ ) was determined for the most accurate models identified through relative variance analysis, as detailed in Table 1. This ratio was graphed against the experimental data's energy range, followed by a polynomial fit. Data points that deviated more than three times the standard deviation were removed. The subsequent set of data underwent a second polynomial fitting. The evaluated cross-section,  $\sigma$  evaluated, was obtained by multiplying the model-calculated cross-section in Eq. (1),  $\sigma_{\text{model}}(E)$ , by the energy-dependent normalization factor,  $f(E)$ , i.e.,

**Table 1** Relative variance analyses of level density models

| CTFGM       | BSFGM      | GSM        |
|-------------|------------|------------|
| 0.412265555 | 0.32666329 | 0.43459015 |

$$\sigma \text{ evaluated} = f(E)\sigma \text{ model}(E) \quad (1)$$

In addition to theoretical analysis, practical production of radionuclides involves several key variables. The size of the reaction cross-section as a function of energy, the energy of the incident particle, the thickness of the target in nuclei per  $\text{cm}^2$ , which will determine the energy of the exit particle, and other parameters are among them, and the flux, which is related to beam current of incoming particles. The following equation provides information on the rate of production Eq. (2);

$$Y(t) = I\rho \frac{N_A}{M} (1 - e^{-\lambda t}) \int_{E_o}^{E_i} S(E)^{-1} \sigma(E) \, dE \quad (2)$$

where  $I$  is beam current,  $\rho$  and  $M$  are the density and molar mass of target material respectively,  $N_A$  is Avogadro number,  $\lambda$  is decay rate,  $t$  is irradiation time,  $E_o$  and  $E_i$  are initial and final energy of the beam,  $S(E)$  is stopping power and  $\sigma(E)$  is the reaction cross-section in Eq. (2).

### 3 Results and discussions

Reaction cross-section, reaction yield, and activation are three important parameters for radioisotope production at cyclotron. In this study production routes and parameters of  $^{211}\text{At}$  were carried out in three stages, which are i) Determining beam energy, ii) Production cross-section calculations, and iii) Activation and Yield calculations.

#### 3.1 Beam energy

When a target is bombarded with charged or uncharged particles, not only one type of nuclear reaction occurs but also multiple nuclear reactions may occur depending on the energy of the incoming particle in the entrance channel. Because most radioisotopes have a shorter half-life, radioisotopic purities are also important for radioisotope production. The beam energy should be chosen in such a way that it does not require complex separation techniques. Selection of the beam energy for maximum reaction cross-section is not always true. All possible nuclear reactions that occurred by bombarding  $^{209}\text{Bi}$  with alphas were calculated to determine the beam energy to produce  $^{211}\text{At}$  of maximum purity. In Fig. 1, reaction cross-section calculations done by using the Two-Component Exciton Model for all possible nuclear reactions have been given. Calculations performed up to 60 MeV alpha energy. Among all possible reactions,  $^{208-211}\text{At}$  are the most probable exit channels. The energy range for the  $^{211}\text{At}$  production is around 20–40 MeV. In this energy region three other radioisotopes, which are  $^{208}\text{Bi}$ ,  $^{210}\text{At}$ , and  $^{212}\text{At}$  are produced. Maximum cross-section energy for  $^{211}\text{At}$  production is approximately 30–31 MeV. In this energy  $^{210}\text{At}$ , which has parent nuclei of  $^{210}\text{Po}$ , has been observed.  $^{210}\text{Po}$  with 138.2 days half-life, is highly toxic. Therefore, 28 MeV was determined for the beam energy selection, where the other reaction cross sections are low.

#### 3.2 Production cross-section calculations

After the beam energy was determined, three different level density models were used to obtain cross-section results that best fit the experimental data. For level density models, CTFGM, BSFGM, and GSM have been chosen because lots of studies have been performed in literature [17, 18, 18–20] by these models for nuclear data evaluations. Two-Component Exciton Model has been

**Fig. 1** Cross-section calculations for the  $^{209}\text{Bi}(\alpha, x)$  reaction

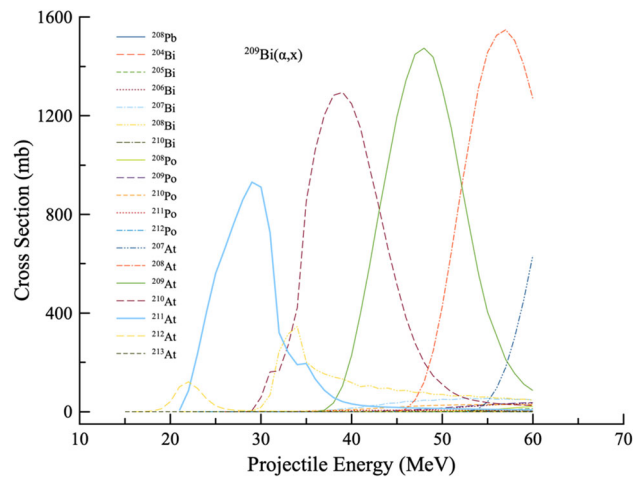


**Fig. 2** Comparisons of calculated cross-section of  $^{209}\text{Bi}(\alpha,2n)^{211}\text{At}$  reaction with the experimental data

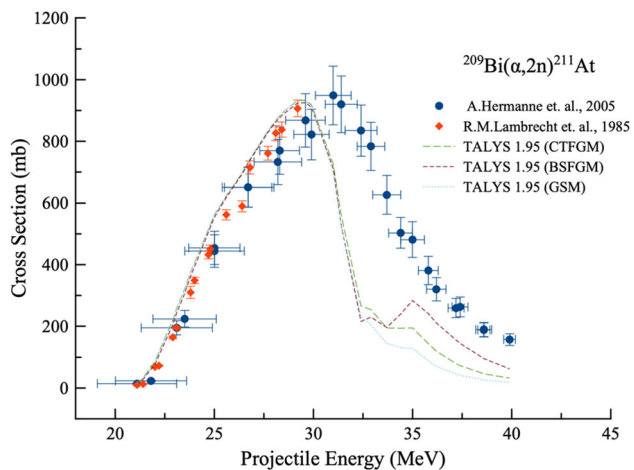
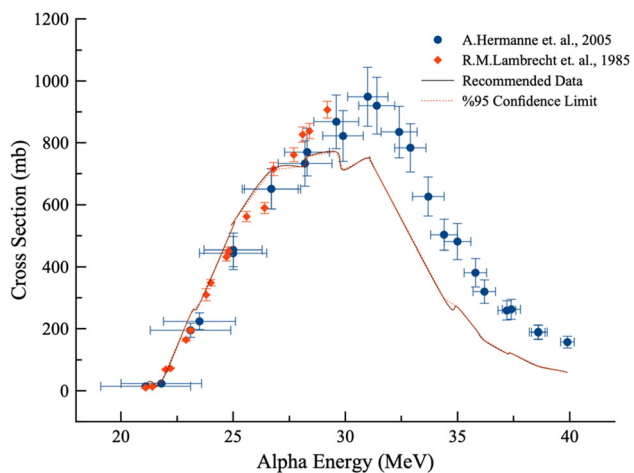


**Fig. 3** Experimental data against the recommended fit for  $^{209}\text{Bi}(\alpha,2n)^{211}\text{At}$  reaction



employed because the pre-equilibrium effects are more dominant for the energy region of  $^{209}\text{Bi}(\alpha,2n)^{211}\text{At}$  reaction. Additionally, relative variance analysis have been carried out to identify the most effective level density models. The comparison of  $^{211}\text{At}$  production cross-section calculations with experimental data of Hermann et al. [21] and Lambrecht et al. [22] have been shown in Fig. 2. The reaction Q value is found to be -20.329 MeV. The level density model findings are in reasonable agreement with the experimental data up to roughly 31 MeV, which can be seen in Fig. 2. After this energy, the theoretical calculations lost their compatibility with the experimental data. Since the beam energy was determined as 28 MeV, the mismatch after 31 MeV was ignored. The BSFGM seems to be the most accurate level density model based on evaluations of relative variance.

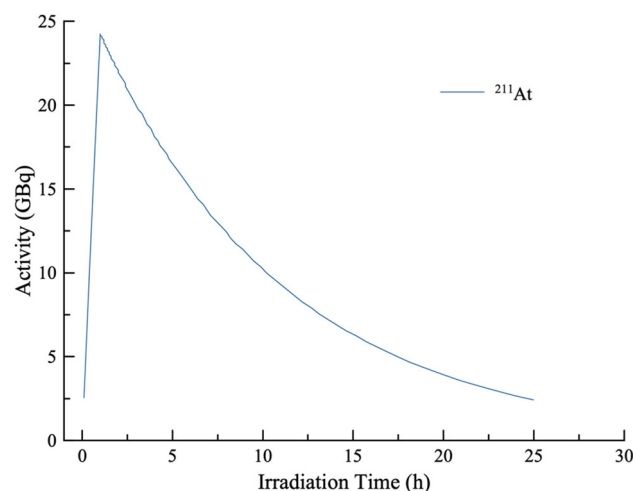
To further validate these findings, the experimental uncertainties were carefully weighted during the polynomial fitting process, ensuring that the final fitted cross sections included 95% confidence limits for both the upper and lower bounds. These results are referred to as the recommended cross-section data. The recommended data with the 95% confidence limit against the experimental data were given in Fig. 3 and Table 2. The confidence intervals provided are calculated concerning the theoretical calculations, offering an indication of the reliability of the recommended data. The narrow confidence intervals around the recommended data suggest a high degree of precision in both the experimental measurements and the theoretical modeling up to 28 MeV. The alignment of the recommended data (solid line) with the experimental points from Hermann et al. [21] and Lambrecht et al. [22] and the accompanying 95% confidence limits (dotted lines) indicates a good fit up to 28 MeV. Table 2 and Fig. 3 provide strong evidence for the selection of 28 MeV as the optimal energy for the reaction under consideration. The narrow confidence intervals up to this energy level reinforce the reliability of the recommended data for practical applications.

### 3.3 Reaction yield and activity calculations

Calculated activity and reaction yield have been shown in Figs. 4 and 5 respectively. The results obtained in the first and second steps of the study were used for activity and reaction yield calculations. BSFGM was been fixed as level density models and alpha beam energy was selected at 28 MeV. Calculation was done for the Irradiation time of 1 h with a beam current of 1 mA. The maximum reaction yield (25.3 GBg/mAh) was found after 0.1 h of irradiation. Thereafter it decreases to 23.21 GBq/mAh after 1 h of irradiation. Activity of  $^{211}\text{At}$  has reached 24.25 GBq after the end of irradiation.

**Table 2** Recommended cross-section data with 95% confidence limit

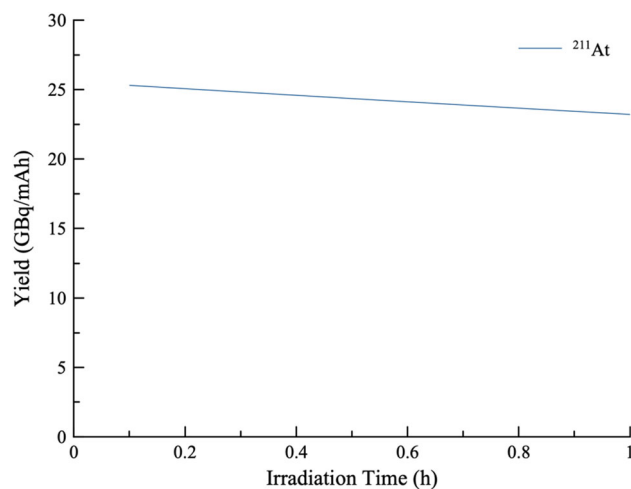
| Energy (MeV) | Cross-section (mb) | %95 Confidence limit (mb) |             |
|--------------|--------------------|---------------------------|-------------|
|              |                    | Upper limit               | Lower limit |
| 21.1         | 17.80              | 17.11                     | 18.48       |
| 21.8         | 29.39              | 28.73                     | 30.05       |
| 23.1         | 246.74             | 246.11                    | 247.37      |
| 23.5         | 281.17             | 280.54                    | 281.80      |
| 25.0         | 530.30             | 529.68                    | 530.91      |
| 25.0         | 542.24             | 541.63                    | 542.86      |
| 26.7         | 711.33             | 710.72                    | 711.95      |
| 28.2         | 724.25             | 723.63                    | 724.87      |
| 28.3         | 755.28             | 754.67                    | 755.90      |
| 29.6         | 770.64             | 770.02                    | 771.26      |
| 29.9         | 712.42             | 711.80                    | 713.04      |
| 31.0         | 751.04             | 750.41                    | 751.66      |
| 31.4         | 703.89             | 703.27                    | 704.51      |
| 34.4         | 297.17             | 296.56                    | 297.79      |
| 35.0         | 269.86             | 269.24                    | 270.47      |
| 35.8         | 199.61             | 199.00                    | 200.23      |
| 36.2         | 162.05             | 161.44                    | 162.67      |
| 37.2         | 120.59             | 119.97                    | 121.21      |
| 37.4         | 120.43             | 119.80                    | 121.06      |
| 38.6         | 78.84              | 78.19                     | 79.49       |
| 39.9         | 58.72              | 58.03                     | 59.41       |

**Fig. 4** Calculated total activity of  $^{211}\text{At}$  vs. irradiation time

A broad range of  $^{211}\text{At}$  labeled chemicals have shown positive results in the treatment of cancer, and the potential benefits of  $^{211}\text{At}$  for targeted alpha particle irradiation have been known for approximately 40 years. The therapeutic radionuclide of greatest interest is  $^{211}\text{At}$  [9, 23]. In addition, the production of  $^{211}\text{At}$  has a low inherent cost as compared to other prospective alpha particle emitters for cancer treatment, such as  $^{225}\text{Ac}$ . In addition, the favorable half-life during treatment is among the advantages of this isotope [9].

The  $\alpha$  particles have cell-killing potency including production and availability limitations. Solutions to this research are currently being investigated for the  $\alpha$ -emitters cross section values, on the other hand, it provided significant results in the calculations of  $^{211}\text{At}$   $\alpha$ -emitters cross-section.

**Fig. 5** Calculated reaction yield vs. irradiation time



#### 4 Conclusion

In this paper, nuclear reaction models have been used to compute the reaction cross-sections of  $^{209}\text{Bi}(\alpha, 2n)^{211}\text{At}$ . For all computations, TALYS 1.95 has been used. The findings have been compared to those from the EXFOR. The outcomes acquired can be summed up as follows;

- (1) Despite the cross-section of  $^{209}\text{Bi}(\alpha, 2n)^{211}\text{At}$  is maximum around 31 MeV, the beam energy is determined as 28 MeV to avoid harmful effects of  $^{210}\text{Po}$ , which is the daughter nuclei of  $^{210}\text{At}$ .
- (2) Reaction cross-section calculations based on pre-equilibrium approximations and level density models have exhibited good harmony using the experimental results up to 31 MeV projectile energy.
- (3) The most compatible level density model is BSFGM based on the experimental results.
- (4) The maximum value of reaction yield is 25.3 GBq/mAh, whereas the maximum activity of  $^{211}\text{At}$  is found to be 24.25 GBq.

**Acknowledgements** The present research received no specific grant from any funding agency in the public, commercial, or not-for-profit sectors. We would like to thank Department of Medical Imaging Techniques at Antalya Bilim University, Department of Biomedical Equipment Technology at Akdeniz University, and Department of Physics at Süleyman Demirel University.

**Funding** Open access funding provided by the Scientific and Technological Research Council of Türkiye (TÜBİTAK).

**Data Availability Statement** No Data associated in the manuscript.

#### Declarations

**Conflict of interest** The authors declare that they have no known conflict of financial interests or personal relationships that could have appeared to influence the work reported in this paper

**Open Access** This article is licensed under a Creative Commons Attribution 4.0 International License, which permits use, sharing, adaptation, distribution and reproduction in any medium or format, as long as you give appropriate credit to the original author(s) and the source, provide a link to the Creative Commons licence, and indicate if changes were made. The images or other third party material in this article are included in the article's Creative Commons licence, unless indicated otherwise in a credit line to the material. If material is not included in the article's Creative Commons licence and your intended use is not permitted by statutory regulation or exceeds the permitted use, you will need to obtain permission directly from the copyright holder. To view a copy of this licence, visit <http://creativecommons.org/licenses/by/4.0/>.

#### References

1. P.J. Blower, A nuclear chocolate box: the periodic table of nuclear medicine. *Dalton Trans.* **44**, 4819–4844 (2015)
2. S. Poty et al.,  $\alpha$ -Emitters for radiotherapy: from basic radiochemistry to clinical studies-part 1. *J. Nucl. Med.* **59**(6), 878–884 (2018)
3. K.E. Baidoo, K. Yong, M.W. Brechbiel, Molecular pathways: targeted alpha-particle radiation therapy. *Clin. Cancer Res.* **19**, 530–537 (2013)
4. G. Sgouros, J.C. Roeske, M.R. McDevitt et al., MIRD pamphlet no. 22 (abridged): radiobiology and dosimetry of alpha-particle emitters for targeted radionuclide therapy. *J. Nucl. Med.* **51**, 311–328 (2010)
5. J.P. Pouget, J. Constanzo, Revisiting the radiobiology of targeted alpha therapy. *Front. Med.* **8**, 692436 (2021)
6. M.A. Walicka, G. Vaidyanathan, M.R. Zalutsky, S.J. Adelstein, A.I. Kassis, Survival and DNA damage in Chinese hamster V79 cells exposed to alpha particles emitted by DNA-incorporated astatin-211. *Radiat. Res.* **150**, 263 (1998)
7. F. Guérard, J.F. Gestin, M.W. Brechbiel, Production of [(211)At]-astatinated radiopharmaceuticals and applications in targeted  $\alpha$ -particle therapy. *Cancer Biother. Radiopharm.* **28**(1), 1–20 (2013)

8. R.H. Larsen, B.W. Wieland, M.R. Zalutsky, Evaluation of an internal cyclotron target for the production of  $^{211}\text{At}$  via the  $^{209}\text{Bi}$  ( $\alpha, 2n$ )  $^{211}\text{At}$  reaction. *Appl. Radiat. Isot.* **47**(2), 135–143 (1996). [https://doi.org/10.1016/0969-8043\(95\)00285-5](https://doi.org/10.1016/0969-8043(95)00285-5)
9. M.R. Zalutsky, M. Pruszynski, Astatine-211: production and availability. *Curr. Radiopharm.* **4**(3), 177–185 (2011)
10. G. Vaidyanathan, M.R. Zalutsky, Astatine Radiopharmaceuticals: Prospects and Problems. *Curr. Radiopharm.* **1**(3), 177 (2008)
11. A. Koning, S. Hilaire, S. Goriely, TALYS-1.95 A Nuclear reaction program, user manual (NRG, The Netherlands), First Edition, 2019.
12. H. Baba, A shell-model nuclear level density. *Nucl. Phys. A* **159**, 625 (1970)
13. A.V. Ignatyuk, G.N. Smirenkin, A.S. Tishin, Phenomenological description of the energy dependence of the level density parameter. *Sov. J. Nucl. Phys.* **21**, 255 (1975)
14. A.V. Ignatyuk, K.K. Istekov, G.N. Smirenkin, The role of collective effects in the systematics of nuclear level densities. *Yad. Fiz.* **29**, 875 (1979)
15. M.N. Aslam, S. Sudar, M. Hussain, A.A. Malik, H.A. Shah, S.M. Qaim, Evaluation of excitation functions of proton and deuteron induced reactions on enriched tellurium isotopes with special relevance to the production of iodine-124. *Appl. Radiat. Isot.* **68**, 1760–1773 (2010)
16. S. Sudar, F. Cserpák, S.M. Qaim, Measurements and nuclear model calculations on proton-induced reactions on  $^{103}\text{Rh}$  up to 40 MeV: evaluation of the excitation function of the  $^{103}\text{Rh}(\text{p}, \text{n})^{103}\text{Pd}$  reaction relevant to the production of the therapeutic radionuclide  $^{103}\text{Pd}$ . *Appl. Radiat. Isot.* **56**, 821–831 (2002)
17. N. Arned, F. Tárkányi, F. Dítroi, S. Takacs, H. Yuki, Activation cross-sections of deuteron induced reactions of natural Ni up to 40 MeV. *Appl. Radiat. Isot.* **82**, 87–99 (2013)
18. İH. Sarpiün, H. Özdogan, K. Taşdöven, H.A. Yalim, A. Kaplan, Theoretical photoneutron cross-section calculations on Osmium isotopes by Talya and Empire codes. *MPLA* **34**(26), 1950210 (2019)
19. M. Şekerci, H. Özdogan, A. Kaplan, Level density model effects on the production cross-section calculations of some medical isotopes via  $(\alpha, xn)$  reactions where  $x = 1, 3$ . *MPLA* **35**(24), 2050202 (2020)
20. M. Şekerci, H. Özdogan, A. Kaplan, An investigation of effects of level density models and gamma-ray strength functions on cross-section calculations for the production of  $^{90}\text{Y}$ ,  $^{153}\text{Sm}$ ,  $^{169}\text{Er}$ ,  $^{177}\text{Lu}$  and  $^{186}\text{Re}$  therapeutic radioisotopes via  $(n, \gamma)$  reactions. *Radiochim. Acta* **108**(1), 11–17 (2020)
21. H. Özdogan, V. Çapalı, A. Kaplan, Reaction cross section stopping power and penetrating distance calculations for the structural fusion material  $^{54}\text{Fe}$  in different reactions. *J. Fusion Energy* **34**(2), 379–385 (2015)
22. H. Özdogan, Y.A. Üncü, M. Şekerci, A. Kaplan, Estimations of level density parameters by using artificial neural network for phenomenological level density models. *Appl. Radiat. Isot.* **169**, 109583 (2021)
23. A. Hermann, F. Tárkányi, S. Takács, Z. Szűcs, Y.N. Shubin, A.I. Dityuk, Experimental study of the cross-sections of  $\alpha$ -particle induced reactions on  $^{209}\text{Bi}$ . *Appl. Radiat. Isot.* **63**(1), 1–9 (2005)
24. R.M. Lambrecht, S. Mirzadeh, Cyclotron isotopes and radiopharmaceuticals—XXXV astatine-211. *Appl. Radiat. Isot.* **36**(6), 443–450 (1985)
25. J. Barbet, J.F. Chatal, F. Gauché, J. Martino, Which radionuclides will nuclear oncology need tomorrow? *Eur. J. Nucl. Med. Mol. Imaging* **33**(6), 627–630 (2006)